

2012

# Decorin Expression, Straw-Like Structure, and Differentiation of Human Costal Cartilage

Michael W. Stacey

*Old Dominion University*, [mstacey@odu.edu](mailto:mstacey@odu.edu)

Janna Grubb

*Old Dominion University*

Anthony Asmar

*Old Dominion University*

Julie Pryor


*Old Dominion University*

Hani Elsayed-Ali

*Old Dominion University*

*See next page for additional authors*

Follow this and additional works at: [https://digitalcommons.odu.edu/bioelectrics\\_pubs](https://digitalcommons.odu.edu/bioelectrics_pubs)

 Part of the [Biomedical Engineering and Bioengineering Commons](#), [Cell and Developmental Biology Commons](#), and the [Musculoskeletal Diseases Commons](#)

---

## Repository Citation

Stacey, Michael W.; Grubb, Janna; Asmar, Anthony; Pryor, Julie; Elsayed-Ali, Hani; Beskok, Ali; Dutta, Diganta; Fecteau, Annie; Werner, Alice; Darby, Dennis A.; and Kelly, Robert, "Decorin Expression, Straw-Like Structure, and Differentiation of Human Costal Cartilage" (2012). *Bioelectrics Publications*. 69.

[https://digitalcommons.odu.edu/bioelectrics\\_pubs/69](https://digitalcommons.odu.edu/bioelectrics_pubs/69)

This Article is brought to you for free and open access by the Frank Reidy Research Center for Bioelectrics at ODU Digital Commons. It has been accepted for inclusion in Bioelectrics Publications by an authorized administrator of ODU Digital Commons. For more information, please contact [digitalcommons@odu.edu](mailto:digitalcommons@odu.edu).

---

**Authors**

Michael W. Stacey, Janna Grubb, Anthony Asmar, Julie Pryor, Hani Elsayed-Ali, Ali Beskok, Diganta Dutta, Annie Fecteau, Alice Werner, Dennis A. Darby, and Robert Kelly



**Decorin Expression, Straw-like Structure, and Differentiation of Human Costal Cartilage.**

Journal:	<i>Connective Tissue Research</i>
Manuscript ID:	GCTS-2012-0023.R1
Manuscript Type:	Original Research
Date Submitted by the Author:	n/a
Complete List of Authors:	<p>Stacey, Michael; Old Dominion University, Frank Reidy Research Center for Bioelectrics                      Grubb, Janna; Old Dominion University, Frank Reidy Research Center for Bioelectrics                      Asmar, Anthony; Old Dominion University, Frank Reidy Research Center for Bioelectrics                      Pryor, Julie; Old Dominion University, Frank Reidy Research Center for Bioelectrics                      Elsayed-Ali, Hani; Applied Research Center,                      Cao, Wei; Applied Research Center,                      Beskok, Ali; Old Dominion University, Institute of Micro and Nanotechnology                      Dutta, Diganta; Old Dominion University, Institute of Micro &amp; Nanotechnology                      Fecteau, Annie; Hospital for Sick Children, Surgery                      Werner, Alice; Children's Hospital of the King's Daughters, Pediatric Pathology                      Darby, Dennis; Old Dominion University, Oceanography and Earth Sciences                      Kelly, Robert; Children's Hospital of the King's Daughters, Pediatric Surgery</p>
Keywords:	pectus carinatum, chest wall deformity, SLRPs, AFM, gene ratio, connective tissue

1  
2  
3  
4  
5  
6  
7  
8  
9  
10  
11  
12  
13  
14  
15  
16  
17  
18  
19  
20  
21  
22  
23  
24  
25  
26  
27  
28  
29  
30  
31  
32  
33  
34  
35  
36  
37  
38  
39  
40  
41  
42  
43  
44  
45  
46  
47  
48  
49  
50  
51  
52  
53  
54  
55  
56  
57  
58  
59  
60

## Decorin Expression, Straw-like Structure, and Differentiation of Human Costal Cartilage.

Stacey MW<sup>1,2</sup>, Grubb J<sup>1</sup>, Asmar A<sup>1</sup>, Pryor J<sup>1</sup>, El-Sayed Ali<sup>3</sup> H, Cao W<sup>3</sup>, Beskok A<sup>4</sup>, Dutta D<sup>4</sup>, Darby DA<sup>5</sup>, Fecteau A<sup>6</sup>, Werner A<sup>7</sup>, Kelly RE Jr<sup>8</sup>.

<sup>1</sup>Frank Reidy Research Center for Bioelectrics, Old Dominion University, Norfolk, VA USA

<sup>2</sup>Department of Pediatrics, Eastern Virginia Medical School, Norfolk VA USA

<sup>3</sup> Applied Research Center, Electrical and Computer Engineering, Old Dominion University, Norfolk, VA

<sup>4</sup>Institute of Micro & Nanotechnology, Old Dominion University, Norfolk, VA

<sup>5</sup>Oceanography and Earth Sciences, Old Dominion University, Norfolk, VA

<sup>6</sup>Division of General Surgery, Hospital for Sick Children, Toronto, Canada.

<sup>7</sup>Dept of Pathology, Eastern Virginia Medical School and Med Director of Laboratories, Children's Hospital of The King's Daughters, Norfolk VA

<sup>8</sup> Department of Surgery, Eastern Virginia Medical School and Pediatric Surgery Division, Children's Hospital of the King's Daughters, Norfolk VA

Corresponding author:

Dr. Michael Stacey, Frank Reidy Research Center for Bioelectrics, 4211 Monarch Way, Suite 300, Norfolk, VA 23508 USA

Email: [mstacey@odu.edu](mailto:mstacey@odu.edu)

Telephone: 757 683 2245

Fax: 757 451 1010

**Running head** Human costal cartilage

**Key Words** Pectus carinatum, chest wall deformities, connective tissue, SLRPs, AFM, gene ratio,

**ABSTRACT**

Costal cartilage is much understudied compared to the load bearing cartilages. Abnormally grown costal cartilages are associated with the inherited chest wall deformities pectus excavatum and pectus carinatum resulting in sunken or pigeon chest respectively. A lack of understanding of the ultrastructural and molecular biology of costal cartilage is a major confounder in predicting causes and outcomes of these disorders. The present study analyzed the structure of marginal human costal cartilage (ribs 6-10) through scanning electron and atomic force microscopy and identified the presence of straw-like structures running longitudinally. We also demonstrated that chondrocytes tend to occur singly or as doublets and that centrally located cells produce high levels of aggrecan compared to more peripherally located cells measured by immunohistochemistry. Gene expression from mRNA extracted from cartilage showed high levels of decorin expression, likely associated with the large, complex tubular structures running through this cartilage type. *COL2A1*, *ACAN* and *TIMP1* also showed higher levels of expression compared to *ACTB*. Analysis of gene expression ratios demonstrate that costal cartilage is under differentiated compared to published ratios for articular cartilage, likely due to the vastly different biomechanical environments of each cartilage type. Further studies need to establish whether findings described here from the costal margins are significantly different to cartilage of the 'true ribs' and how these values change with age.

## INTRODUCTION

Costal cartilage, a type of hyaline cartilage, connects each of ribs 1-5 to the sternum and ribs 6-10, which are fused, to the sternum as the costal margin. They remain cartilaginous throughout life and provide both strength and flexibility to the chest wall. Disorders of the chest wall can cause significant disfigurement with associated cardiac, pulmonary, and psychological manifestations and are classified as sunken chest (pectus excavatum, PE) or pigeon chest (pectus carinatum, PC) [1]. The costal cartilages of these patients are described as abnormally grown and weak. Disorders of costal cartilage are common, affecting approximately 1/400-1/1,000 individuals, show complex inheritance patterns in families, and affect primarily males (M4:F1) [2, 3, 4, 5]. Chest wall deformities are phenotypically variable and surgical repair outcomes can be unpredictable. The basic molecular characteristics that define a healthy human costal cartilage are largely unknown, and a lack of understanding of the ultrastructural and molecular biology of costal cartilage is a major confounder in predicting outcomes and causes chest wall deformities.

Recent work [6] described a decrease in the biomechanical stability of costal cartilage in pectus excavatum patients and suggested a disorderly arrangement and distribution of collagen fibers. Other authors have suggested that atypical collagen fibers may be implicated in chest wall deformities [7, 8]. The arrangement of collagen fibers in costal cartilage has not been described in detail; however, highly ordered fiber formation was described [9] in the surrounding perichondrium. Growth of human costal cartilage chondrocytes *in vitro* shows high levels of *COL2A1* and *ACAN* expression and low levels of *COL1A1* at low culture passage, typical of a differentiated cell [10]. Differences in the variable number of tandem repeat units of chondroitin sulphate attachment sites were observed in *ACAN* with significantly more repeats (27) being present in patients with chest wall deformities [11].

TGF $\beta$ 1 signaling plays a key role in cartilage growth and ECM turnover. Cells are extremely sensitive to levels of TGF $\beta$ 1 and, therefore, regulation of this growth factor is important in normal growth and development. Genes activated via TGF $\beta$  pathways include *SOX9*, a major transcription factor of chondrocyte differentiation and regulator of

1  
2  
3  
4  
5  
6  
7  
8  
9  
10  
11  
12  
13  
14  
15  
16  
17  
18  
19  
20  
21  
22  
23  
24  
25  
26  
27  
28  
29  
30  
31  
32  
33  
34  
35  
36  
37  
38  
39  
40  
41  
42  
43  
44  
45  
46  
47  
48  
49  
50  
51  
52  
53  
54  
55  
56  
57  
58  
59  
60

*ACAN* and *COL2A1* expression. In addition, *TIMP1*, a regulator of the matrix metalloproteinase's (MMP 8 and 13), is positively regulated by the TGFβ1 pathway [12].

Small leucine-rich proteoglycans (SLRPs) are small proteoglycans that are highly expressed in cartilage. Regulation of collagen fibrillogenesis is an important function shared by many SLRPs, and null mutations have been shown to lead to abnormal collagen architecture in mice [13]. Additionally, SLRPs mediate cell metabolism by binding to growth factors, including members of the superfamily TGFβ1 [14]. The causes of PE and PC are unknown; however, SLRPs can regulate ECM growth and fibrillogenesis by controlling TGFβ availability, suggesting a mechanistic role for SLRPs in these disorders. Biglycan deficiency has been shown to cause spontaneous aortic dissection and rupture in mice [15], and is also a characteristic of Marfan syndrome, a syndrome known to exhibit chest wall deformities. Decorin function is consistent with functions related to fibrillogenesis [16, 17]. A critical concept of SLRP function is compensation of one SLRP function over another. In the absence of biglycan, decorin is up-regulated and, therefore, differences in gene expression ratios may be apparent. Our central hypothesis is that abnormal expression of *BGN* and *DCN* will be observed in patients with chest wall deformities.

A thorough knowledge on the expression patterns of genes responsible for chondrogenesis in costal cartilage would provide insights into the role of these proteins in chest wall deformities and offer a biological rationale for the variability observed in outcome of surgery [18, 19, 20]. The objective of this study was to identify ultrastructural morphology and protein localization, investigate relative levels of expression of key genes required for chondrogenesis, and compare changes in normal costal cartilage and chest wall deformity.

## MATERIALS AND METHODS

### 2.1 Subjects

Human costal cartilage was obtained from 4 patients with pectus carinatum severe enough to warrant surgical repair. Informed consent was obtained following IRB approval of the protocol at Eastern Virginia Medical School. The IRB protocol currently prevents disclosure of many clinical features, and thus close correlation of clinical

1  
2  
3 phenotype with expression is not possible. Costal cartilage samples were collected from  
4 ribs 6-8 at surgery.. Experiments were performed on the round, rod-like, mid-sections of  
5 cartilage. All patients were male, with an age range of early teen to early 20's.  
6  
7

8 Apparently normal costal cartilage was obtained from an age-matched-control, a 15 year  
9 old male and processed within 24 hours. All samples were snap frozen in liquid nitrogen  
10 and stored at -80°C until use.  
11  
12

## 13 **2.2 Ultrastructural analysis**

14 Scanning electron microscopy (SEM) is a well-described technique employed for  
15 ultrastructural studies of cells and tissues. Cartilage, samples were cut into small sections  
16 approximately 3mm thick, washed three times in Sorenson's buffer and digested at 37°C  
17 for 48 hours in trypsin (1mg/ml) and hyaluronidase (1mg/ml) in Sorenson's buffer [21].  
18 Samples were washed thoroughly in PBS and fixed in 2.5% glutaraldehyde in phosphate  
19 buffered saline for 2.5 hours. Samples were rinsed in deionized water, dehydrated  
20 through an ethanol series, dried and mounted on carbon discs, gold sputtered, and  
21 examined using a JSM-6060LV SEM (JEOL, Tokyo, Japan) operating at 5 keV to  
22 minimize sample damage. Images were captured electronically and fiber measurements  
23 made using Image J software.  
24  
25  
26  
27  
28  
29  
30  
31  
32

## 33 **2.3 Atomic Force Microscopy (AFM)**

34 Collagen straws were released from small pieces of tissue by brief homogenization and  
35 digestion with 0.1mg/ml hyaluronidase and 0.1mg/ml trypsin in Sorenson's buffer.  
36 Samples were fixed in ice cold acetone and fiber diameters measured using a Nanonics  
37 Multiview-4000 multi-probe AFM.  
38  
39  
40  
41

## 42 **2.4 Immunohistochemistry**

43 Confirmation of aggrecan gene expression and protein distribution were made by  
44 immunohistochemistry. Frozen cartilage samples were mounted in CRYO-OCT  
45 Compound (Tissue-Tek, CA USA) and sections (5µm) generated using a Microm  
46 HM525 cryostat. Sections were fixed in ice-cold acetone. Blocking, incubation with  
47 primary and secondary antibodies and washing were performed following manufacturer's  
48 guidelines for each antibody. Tissues were incubated with a mouse monoclonal antibody  
49 specific for aggrecan (sc-73693, Santa Cruz, Santa Cruz, CA). The antibody was raised  
50 against recombinant aggrecan from human origin Negative controls were produced using  
51  
52  
53  
54  
55  
56  
57  
58  
59  
60



1  
2  
3 normal mouse IgG included in the ImmunoCruz mouse LSAB staining system (sc-2050,  
4 Santa Cruz). Electronic images were captured using a CCD camera through an Olympus  
5 BX51 with Metamorph and Image J software for semi and quantitative analysis of protein  
6 deposition.  
7  
8  
9

## 10 **2.5 Chondrocyte distribution**

11  
12 Cartilage consists mainly of proteoglycans and collagens, with chondrocytes sparsely  
13 distributed throughout the matrix. We catalogued the distribution pattern of 586 and 999  
14 chondrocytes in transverse sections of costal cartilage from PC3 and Con3 respectively,  
15 through an Olympus BX51 microscope, as groups of 1-4+ cells per cluster located  
16 interiorly or peripherally. Interior cells were within the strongly expressing aggrecan  
17 region, and peripheral cells outside.  
18  
19  
20  
21  
22

## 23 **2.6 Reverse Transcription and Real-Time PCR Analysis**

24  
25 Cartilage was removed from -80°C and transverse sections cut at approximately 3-5mm  
26 on dry ice and placed into RNALater (Qiagen, CA USA). Samples were quickly weighed  
27 and approximately 100mg of costal cartilage was ground to a powder with a liquid  
28 nitrogen immersed pestle and mortar. RNA was isolated and genomic DNA eliminated  
29 by completing RNA extraction using a RNeasy Plus Mini Kit and RT-First Strand Kit  
30 (Qiagen, CA USA). All polymerase chain reactions (PCR) were performed on a BioRad  
31 CFX96 system in 25µl reactions using SYBR green detection (Qiagen, CA USA). Gene  
32 expression by PCR was performed on genes described in Table 1, all compared to the  
33 housekeeping gene *ACTB*. All primers were from Qiagen, CA USA. The reaction  
34 conditions were identical for all primers, 95°C for 10 minutes, then 40 rounds of 95°C for  
35 15 seconds and 60°C for 60 seconds. Reaction specificities were assessed with a melt  
36 curve of 65°C to 95°C in 0.2°C increments. All experiments were in triplicate and  
37 performed with positive and negative controls. At least two independent extractions were  
38 included from samples stored at 4°C in RNALater. Data were standardized to  
39 housekeeping *ACTB* values for all samples using the delta Ct method.  
40  
41  
42  
43  
44  
45  
46  
47  
48  
49  
50

## 51 **2.7 Statistical Analysis**

52  
53 Statistical analysis was performed using Student t-test to determine significance between  
54 sample and control means. For all tests,  $p < 0.05$  indicated the difference as significant.  
55  
56  
57  
58  
59  
60

## RESULTS

### 3.1. Electron Microscopy and AFM

Costal cartilage is a much understudied tissue type, both ultra structurally and genetically. We provide a first description of these properties in samples of human costal cartilage. Figures 1a and 1b are representative SEM images of a transverse cross-section of costal cartilage taken from a mid-section. Figure 1a shows a fracture in the cartilage, estimated as the inner-middle zone, exposing collagen fibers of approximately 600nm diameter. Fibers are assembled into extremely large complexes of many  $\mu\text{m}$  (arrowed) that run parallel to the length of the cartilage. Figure 1b is a higher magnification of the boxed area and shows that each fiber forms a nanostraw of approximately 650nm external diameter and 250nm internal lumen diameter. Images of longitudinal sections show a well-defined organization of collagen fibers approximately 20 $\mu\text{m}$  diameter and cellular lacunae (Figure 1c). We measured the diameters from 150 clearly defined fibers from SEM images (Table 2) and found that most were in the range from 0.1-100  $\mu\text{m}$ . The smallest (<0.1 $\mu\text{m}$ ) would most-likely represent the collagen fibrils, the midsize (~1 $\mu\text{m}$ ) would represent the “microtubes” and the largest (~100 $\mu\text{m}$ ) would be large fascicle-like structures. Cartilage homogenization and digestion released nanostraw fibers and allowed further characterization by AFM. Figure 1d shows an AFM image of branching/splitting fibers with a maximum diameter of approximately 740nm. Clearly, costal cartilage has large fiber dimensions with complex structures formed through finely tuned fibrillogenesis.

### 3.2 Aggrecan immunohistochemistry

Aggrecan deposition from cells appeared to be a function of location. Figure 2 shows a representative cross-section of costal cartilage with cells located centrally exhibiting intense aggrecan staining (A) compared to the more peripherally located cells (B) and outer most cells (C). Interestingly, we were able to show increased levels of sodium ions in the same central region by electron probe microanalysis (EPMA, supplemental figure), showing that positively charged ions were drawn in to achieve electroneutrality.

### 3.3 Chondrocyte distribution

The organization of chondrocytes in cartilage is not considered to be random, and different cartilage types have different configurations of singles, pairs, clusters or strings

of cells. The percentage number of cell clusters observed in the interior was 1 cell (68.5% and 60.2%), 2 cells (23% and 27.3%), 3 cells (4.3% and 10.1%) and 4+ cells (4.2% and 2.4%) respectively for PC3 and Control. For peripherally located cells, observed clusters were 1 cell (86.9% and 73.0%), 2 cells (12.6% and 19.7%), 3 cells (0.5% and 5.5%) and 4+ cells (0% and 1.8%) respectively for PC3 and Control. There is a trend towards higher cell clusters in the interior; however, there appears to be no differences in cell distribution between PC3 and age-matched control.. No strings were observed.

### 3.4 Gene expression

Due to the unusual structure of costal cartilage we undertook analysis of gene expression to determine presence of the main constituents of cartilage; collagen type II, and the large aggregating proteoglycan, aggrecan. We also examined other genes that play a role in growth, structure and differentiation of cartilage. *BGN*, *NYX*, *CACNA1F* and *TIMP1* were of interest because these genes are located on the human X-chromosome, where affected individuals are predominantly male and possess only a single X-chromosome [2, 3].

Costal cartilage from individuals with chest wall deformities is described as abnormally grown and weak. Typically, surgical repair takes place during teenage years to early 20's. Phenotypically, there is considerable variation of the clinical condition of PC, reflecting the complex nature and inheritance observed in these families. Variation in gene expression between samples is, therefore, expected; however, it is unknown whether the expression of matrix genes will be affected by surgical procedures. We compared gene expression of 4 patients with pectus carinatum to an age-matched-control. Table 3 shows *COL2A1*, *DCN*, *ACAN*, and *TIMP1* are all highly expressed compared to *ACTB*. Sample variation was noted, although, as expected, *COL2A1* was expressed to the highest level in all samples.

Compared to control, PC1 showed significant reduction in expression of *DCN* ( $p<0.001$ ) and *TIMP1* ( $p<0.001$ ). PC3 showed significantly lower expression of *COL2A1* ( $p<0.001$ ) and like PC4, both showed decreased expression of *ACAN* ( $p<0.03$  and  $p<0.024$ , respectively). PC4 also showed significantly higher expression of *TIMP1* ( $p<0.001$ ) and decreased expression of *BGN* ( $p<0.04$ ). PC2 showed significant reduction in expression of *COL2A1* ( $p<0.01$ ), *DCN* ( $p<0.0002$ ), *TIMP1* ( $p<0.001$ ), *BGN* ( $p<0.03$ )

1  
2  
3 and *FBNI* ( $p < 0.01$ ). This sample, like all PC samples, was immediately processed from  
4 the operating room, although results suggest possible degradation of this sample.  
5  
6

7 Many patients with chest wall deformities are considered Marfanoid-like [22]  
8 without fulfilling all criteria for diagnosis of Marfan syndrome, including mutations of  
9 the fibrillin-1 gene. The expression of this gene was not significantly different between  
10 control and patients, with the exception of PC2 ( $p < 0.01$ ). Expression of the X-linked  
11 genes *NYX* and *CACNA1F* was not detected in any samples. Overall, deregulation of  
12 *TIMPI* expression was evident in 3/4 PC samples, and expression of *DCN* was  
13 significantly lower in 2/4, suggestive of roles for fibrillogenesis and matrix turnover. The  
14 differentiation status of cartilage can be equated to the ratio of *COL2A1*, present in  
15 differentiated cartilage, to *COL1A1*, present at higher levels in more undifferentiated  
16 cartilage. We compared ratios of gene expression to published data. Ratios of the  
17 differentiation markers *COL2A1:ACAN* and *COL2A1:COL1A1* are low in PC patients  
18 and control (Table 4) compared to rabbit articular cartilage (1090 and 1790, respectively)  
19 but both are highly comparable to the nucleus pulposus region of lumbar discs (23 and  
20 930 respectively), [23]. The ratios of *ACAN:COL1A1* fall between those reported for  
21 fully differentiated rat chondrosarcoma cells (78.4) and dedifferentiated chondrocytes  
22 cultured from costal cartilage (4.6) [24]. A high expression ratio of *COL2A1:COL1A1*  
23 (294.6) in human articular cartilage has been reported [25], but here results are referenced  
24 to *GAPDH* rather than *ACTB*. Overall, these results suggest costal cartilage is at an  
25 intermediate stage of differentiation and likely represents the different functional  
26 requirements of this tissue compared to articular cartilage. Small differences exist  
27 between patients and between patients and control (Table 4), suggesting that gene ratios  
28 measured here are not major contributors to chest wall abnormalities in these samples.  
29 Interestingly, *DCN* is expressed at high levels compared to *BGN*. As well as binding  
30 growth factors, both SLRPs have a role in fibrillogenesis and were hypothesized to play a  
31 role in the etiology of chest wall deformities. The high *DCN/BGN* ratio strongly suggests  
32 the importance of decorin expression in costal cartilage morphology. Decorin is present  
33 at high levels during tendon (fibro-cartilage) development and persists until thick fibers  
34 are formed [26], thus parallels with costal cartilage (hyaline cartilage) are apparent.  
35  
36  
37  
38  
39  
40  
41  
42  
43  
44  
45  
46  
47  
48  
49  
50  
51  
52  
53  
54  
55  
56  
57  
58  
59  
60

## DISCUSSION

Costal cartilage is a much understudied cartilage where deformities have significant clinical consequences. A lack of understanding of molecular and ultrastructural properties hampers understanding events leading to these disorders. The present study compared relative gene expression of major genes of chondrogenesis from patients with pectus carinatum to an age-matched-control to answer questions relating to maintenance and differentiation. Perhaps the most important observations are 1) the longitudinal straw-like arrangement of collagen fibers, 2) the centrally located deposition of aggrecan, 3) the high level of decorin expression, and 4) gene ratios indicating under differentiation compared to articular cartilage.

The ultrastructural electron microscopy images show that human costal cartilage is unlike other cartilage types. Images appear to show that individual fibers are assembled to collectively form very thick, fascicle structures appearing to consist of large numbers of collagen nanostraws that run parallel along the cartilage length. A similar observation of collagen tubules in juvenile rabbit tibia articular cartilage was reported [27], but this is the first report in human costal cartilage. The cartilage template of long bones is similar to costal cartilage in that they are both long, thick, rod-like structures and, therefore, although functionally different, ultrastructural similarities may be expected in response to cell maintenance and collagen fiber deposition under these conditions.

The morphological form of costal cartilage and how this relates to function is currently unknown. The presence of straw-like structures may provide strength and a means of gas and nutrient exchange to cells by fluid flow whose movement is dependent upon cartilage movement during breathing. Costal cartilage can be nearly 1cm diameter, outside of the range of diffusion to maintain centrally located cells [28]. Hypoxia or low pH has been shown to act as a trigger for aggrecan and collagen type II production through induction of hypoxia inducible factor 1- $\alpha$  and *SOX9*, as well as inhibit *COL1A1* expression [29, 30]. Similarities with inter vertebral discs are noteworthy. Cells embedded within the centrally located nucleus pulposus experience hypoxia and express aggrecan under the regulation of the hypoxia induced P13K/AKT signaling pathways via modulation of *SOX9* [31]. It appears that as cells become centrally located

1  
2  
3 they experience hypoxia and lower pH. *ACAN* expression is induced with cationic uptake  
4 that we confirmed by Electron Probe Micro Analysis.  
5  
6

7 Few studies have been undertaken on chondrocyte distribution within cartilage,  
8 yet cell density and arrangements are considered to be critical to function. Cellular  
9 clusters [32], pairs [33], and rows [34], have been reported. A more extensive study [35]  
10 in the superficial zone of articular cartilage identified complex patterns that appear to be  
11 location specific. A spatial relationship between collagen fiber alignment and cellular  
12 organization was suggested [34], with chondrocytes running parallel to adjacent fibers.  
13 Longitudinally, we also note the presence of lacunae between the large fibrous structures.  
14 The predominance of single and doublets in costal cartilage suggests cells undergo  
15 relatively few divisions. The absence of extensive strings and clusters is likely due to the  
16 different biomechanical forces experienced by costal cartilage compared to cartilage  
17 covering ball and socket joints.  
18  
19

20 SLRPs play an important role in fibrillogenesis and shape the architecture and  
21 mechanical properties of the collagen matrix. SLRP-deficient animals exhibit a wide  
22 array of diseases, mostly resulting from abnormal fibrillogenesis [13]. We examined the  
23 expression of three SLRPs; *DCN* and the X-linked genes *BGN* and *NYX*. *NYX* expression  
24 was not detected in any samples of costal cartilage and likely does not play a role in  
25 chondrogenesis. *DCN* has a role in modulating cartilage fibril growth, thickness, and  
26 orientation. Indeed, *DCN* deficiency introduces tissue-specific variations in range, mean,  
27 and distribution of collagen fibril diameters compared to wild-type. Interestingly, *DCN*  
28 deficiency also leads to random orientation of collagen fibrils in periodontal ligament  
29 instead of the usual parallel orientation [36]. Regional variation in localization of  
30 proteoglycans decorin, biglycan, and aggrecan has been reported in tendon, with decorin  
31 highest in regions of greatest tensile strength [37]. However, tensile strength of costal  
32 cartilage appears to reduce as it matures from childhood to teenage/early twenties years  
33 [38], suggesting rearrangement of collagen fibers with age that may be proteoglycan  
34 mediated. The highly aligned collagen fibers observed in costal cartilage show  
35 similarities to the aligned fibers of tendon. The hierarchical assembly of collagen fibers in  
36 tendon is a multistep process leading to the mature tissue [39]. Briefly, collagen fibril  
37 intermediates are assembled and undergo linear and lateral growth. Intercalation of fibrils  
38  
39  
40  
41  
42  
43  
44  
45  
46  
47  
48  
49  
50  
51  
52  
53  
54  
55  
56  
57  
58  
59  
60

1  
2  
3 is necessary for growth resulting in mature fibers and fibrils necessary for mechanical  
4 integrity. The interactions with fibril associated collagens and SLRPs have been  
5 implicated in the form and function of mature tendon. In costal cartilage an additional  
6 layer of complexity in the formation of tubules is intriguing, and suggests, by the high  
7 level of *DCN* expression, that decorin is crucial in this morphology.  
8  
9

10  
11  
12 The relative expression of genes expressed as a ratio has been used to determine  
13 differentiation status of cartilage where *COL2A1* and *ACAN* are highly expressed  
14 compared to *COL1A1*. This ratio decreases rapidly as chondrocytes dedifferentiate *in*  
15 *vitro*. Adaption of tissue to its mechanical constraints leads to different qualitative  
16 compositions. Costal cartilage exhibits a phenotype consistent with cartilage, with high  
17 *COL2A1/COL1A1*, *COL2A1/ACAN* and *ACAN/COL1A1* ratios, although *COL2A1/ACAN*  
18 and *COL2A1/COL1A1* ratios were considerably lower than rabbit articular cartilage also  
19 normalized to *ACTB* [24] suggesting *COL2A1* expression may be reduced. Expression  
20 levels in costal cartilage are closer to those reported in the nucleus pulposus of lumbar  
21 discs than to articular cartilage. Both nucleus pulposus and costal cartilage expression  
22 levels likely represent the functional requirements of their respective mechanical loads  
23 that are considerably different to that experienced in articular cartilage.  
24  
25

26  
27  
28 The present study has uncovered a new dimension of complexity that has not  
29 previously been reported. The study here describes findings that are generated from  
30 samples of costal cartilage that are generally removed at surgery, ribs 6-8. Although the  
31 current study has relatively few samples we feel that the overall results indicate that there  
32 are several important features unique to costal cartilage. Future work will examine  
33 variations along and between different ribs to more closely correlate variations of  
34 functions that may occur within the environment of the chest wall. Connective tissue  
35 gene arrays will allow analysis of many more genes simultaneously correlated to clinical  
36 picture. The etiology of chest wall deformity is complex. Changed growth characteristics  
37 of costal cartilage in patients may be a secondary characteristic due to external factors.  
38 Alternatively deformed cartilage may be intrinsic due to the inherited, albeit complex,  
39 nature of these disorders. Future work will aim to clarify these discrepancies.  
40  
41  
42  
43  
44  
45  
46  
47  
48  
49  
50  
51  
52  
53  
54  
55

## 56 **Acknowledgments**

57  
58  
59  
60

1  
2  
3 We thank Dr M. Young, National Institute of Dental and Craniofacial Research, NIH and  
4  
5 Dr C. Osgood, College of Sciences, Old Dominion University for critical review of this  
6  
7 manuscript, and Old Dominion University Office of Research for seed funding grant.  
8  
9

10 **Declaration of interest:** The authors have declared no conflict of interest.  
11  
12  
13  
14  
15  
16  
17  
18  
19  
20  
21  
22  
23  
24  
25  
26  
27  
28  
29  
30  
31  
32  
33  
34  
35  
36  
37  
38  
39  
40  
41  
42  
43  
44  
45  
46  
47  
48  
49  
50  
51  
52  
53  
54  
55  
56  
57  
58  
59  
60

For Peer Review Only



## References

- [1] Kelly RE, Shamberger RC, Mellins RB, Mitchell KK, Lawson ML, Oldham K, Azizkhan RG, Hebra AV, Nuss D, Goretsky MJ, Sharp RJ, Holcomb GW, Shim WKT, Megison SM, Moss RL, Fecteau AH, Colombani PM, Bagley TC and Moskowitz AB. Prospective Multicenter Study of Surgical Correction of Pectus Excavatum: Design, Perioperative Complications, Pain, and Baseline Pulmonary Function Facilitated by Internet-Based Data Collection. *J. Am. College of Surgeons.* (2007) 205: 205-216
- [2] Horth L, Stacey MW, Benjamin T, Segna K, Proud VK, Nuss D, Kelly RE. Genetic analysis of inheritance of *Pectus excavatum*. *J. Pediatric Genetics.* (2012) In press
- [3] Creswick H, Stacey M, Kelly R, Burke B, Gustin T, Mitchell K, Nuss D, Harvey H, Croitoru D, Goretsky M, Vasser E, Fox P, Goldblatt S, Tabangin M, Proud V. Family studies on the inheritance of pectus excavatum. *J. Pediatr. Surg.* (2006) 41:1699-1703
- [4] Leung AK, Hoo JJ. Familial congenital funnel chest. *Am. J. Med. Genet.* (1987). 26: 887-890
- [5] Sugiura, Y. A family with funnel chest in three generations. *Jpn. J. Hum. Genet.* (1977). 22: 287-289.
- [6] Feng J, Hu T, Liu W, Zhang S, Tang Y, Chen R, Jiang X, Wei F. The biomechanical, morphologic, and histochemical properties of the costal cartilages in children with pectus excavatum. *J. Pediatr. Surg.* (2001). 36: 1770-1776.
- [7] Rupprecht H, Hümmer, HP. Stöß, H. Waldherr T. Pathogenesis of the Chest Wall Deformities - Electron Microscope Studies and Analysis of Trace Elements in the Cartilage of the Ribs. *Eur J Pediatr Surg* (1987). 42(4): 228-229
- [8] Fokin AA, Nury M, Steuerwald M, Ahrens William A, Allen KE. Anatomical, Histologic, and Genetic Characteristics of Congenital Chest Wall Deformities. *Semin Thorac Cardiovasc Surg.* (2009). 21(1):44-57
- [9] Forman JL, del Pozo de Dios E, Dalmases CA, Kent RW. The contribution of the perichondrium to the structural mechanical behavior of the costal-cartilage. *J. Biomech. Eng.* (2010) 132; /094501 doi: 10.1115/1.4001976
- [10] Zhang Y, Chai G, Liu W, Cui L, Cao YL. Age-related changes in growth and metabolism function of human costal chondrocytes cultured in vitro. *Zhonghua Zheng Xing Wai Ke Zhi* (2004) 20; 372-376
- [11] Stacey M, Neumann S, Dooley A, Segna K, Kelly R, Nuss D, Kuhn A, Goretsky M, Fecteau A, Pastor A, Proud V. Variable Number of Tandem Repeat Polymorphisms (VNTRs) in the *ACAN* Gene Associated with Pectus Excavatum. *Clin. Genet.* (2010). 78;502-504

- 1  
2  
3 [12] El Mabrouk M, Qureshi HY, Li QW, Sylvester J, Zafarullah M. Interleukin-4  
4 antagonizes oncostatin M and transforming growth factor beta-induced responses in  
5 articular cartilage. *J. Cell. Biochem.* (2008).103: 588-597.  
6  
7  
8 [13] Ameye L, Young MF. Mice deficient in small leucine-rich proteoglycans: novel in  
9 vivo models for osteoporosis, osteoarthritis, Ehlers-Danlos syndrome, muscular  
10 dystrophy, and corneal diseases. *Glycobiology* (2002).12: 107R-116R.  
11  
12 [14] Hildebrand A, Romaris M, Ramussen LM, Heingard D, Twardzik DR, Border WA,  
13 Ruoslahti E Interaction of the small interstitial proteoglycans biglycan, decorin and  
14 fibromodulin with transforming growth factor  $\beta$ . *Biochem. J.* (1994). 302: 527-534  
15  
16 [15] Heegaard AM, Corsi A, Danielsen CC, Nielsen KL, Jorgensen HL, Riminucci M,  
17 Young MF, Bianco P. Biglycan Deficiency Causes Spontaneous Aortic Dissection and  
18 Rupture in Mice. *Circulation.* (2007);115:2731-2738.  
19  
20 [16] Bianco P, Fisher LW, Young MF, Termine JD, Robey PG. Expression and  
21 localization of the two small proteoglycans biglycan and decorin in developing human  
22 skeletal and non-skeletal tissues. *J. Histochem. Cytochem.* (1990). 38: 1549-1563  
23  
24 [17] Kalamajski S, Oldberg A. The role of small leucine-rich proteoglycans in collagen  
25 fibrillogenesis. *Matrix Biol.* (2010) 29; 248-253  
26  
27 [18] Antonoff MB, Saltzman DA, Hess DJ, Acton RD. Retrospective review of  
28 reoperative pectus excavatum repairs. *J. Pediatr Surg.* (2010). 45(1):200-5.  
29  
30 [19] Bouchard S, Hong AR, Gilchrist BF, Kuenzler KA. Catastrophic cardiac injuries  
31 encountered during the minimally invasive repair of pectus excavatum. *Semin. Pediatr.*  
32 *Surg.* (2009) 18(2):66-72.  
33  
34 [20] Swanson JW, Colombani PM. Reactive pectus carinatum in patients treated for  
35 pectus excavatum. *J. Pediatr. Surg.* (2008). 43(8):1468-73.  
36  
37 [21] Stolz M, Gottardi R, Raiteri R, Miot S, Martin I, Imer R, Staufer U, Raducanu A,  
38 Duggelin M, Baschong W, Daniels AU, Friederich NF, Aszodi A & Aebi U. Early  
39 detection of aging cartilage and osteoarthritis in mice and patient samples using atomic  
40 force microscopy. *Nature Nanotechnology* (2009) 4; 186-192  
41  
42 [22] Redlinger RE Jr., Rushing GD, Moskowitz AD, Kelly RE, Jr., Nuss D, Kuhn A,  
43 Obermeyer RJ, Goretsky MJ. Minimally invasive repair of pectus excavatum in patients  
44 with Marfan Syndrome and Marfanoid features. *J. Pediatr. Surg.* (2010). 45(1): 193-199  
45  
46 [23] Clouet J, Grimandi G, Pot-Vaucel M, Masson M, Fellah HB, Guigand L, Chereil Y,  
47 Bord E, Rannou F, Weiss P, Guicheux J and Vinatier C. (2009). Identification of  
48 phenotypic discriminating markers for intervertebral disc cells and articular  
49 chondrocytes. *Rheumatology* (2009) 48 (11): 1447-1450.  
50  
51  
52  
53  
54  
55  
56  
57  
58  
59  
60

1  
2  
3  
4  
5 [24] McAlinden A, Havlioglu N, Liang L, Davies SR, Sandell LJ. Alternative Splicing of  
6 Type II Procollagen Exon 2 Is Regulated by the Combination of a Weak 5' Splice Site  
7 and an Adjacent Intronic Stem-loop Cis Element. *J. Biol. Chem.* (2005). 280; 32700-  
8 32711  
9

10 [25] Martin I, Jakob M, Schafer D, Dick W, Spagnoli G, Heberer M. Quantitative  
11 analysis of gene expression in human articular cartilage from normal and osteoarthritic  
12 joints. *Osteoarthr. Cartilage* (2001) 9; 112-118  
13

14 [26] Kalamajski S, Oldberg A. The role of small leucine-rich proteoglycans in collagen  
15 fibrillogenesis. *Matrix Biology* (2010) 29; 248-253  
16  
17

18 [27] Gwynn AP, Wade S, Kääh MJ, Owen GR, Richards RG. Freeze-substitution of  
19 rabbit tibial articular cartilage reveals that radial zone collagen fibers are tubules. *J.*  
20 *Microsc.* (2000) 197; 159-172  
21  
22

23 [28] Gibson JS, Milner PI, White R, Fairfax TP, Wilkins RJ. Oxygen and reactive oxygen  
24 species in articular cartilage: modulators of ionic homeostasis. *Pflugers Arch.* (2008) 455;  
25 563-573  
26  
27

28 [29] Duval E, Leclercq S, Elissalde JM, Demoor M, Galera P, Boumediene K. Hypoxia-  
29 inducible factor 1 $\alpha$  inhibits the fibroblast-like markers type I and type III collagen during  
30 hypoxia-induced chondrocyte redifferentiation. *Arthritis Rheum.* (2009) 60; 3038-3048  
31  
32

33 [30] Das RHJ, van Osch GJVM, Kreukniet M, Oostra J, Weinans H, Jahr H Effects of  
34 individual control of pH and hypoxia in chondrocyte culture. *J. Orthop. Res.* (2010). 28;  
35 537-545  
36

37 [31] Chin-Chang Cheng, Yoshiyasu Uchiyama, Akihiko Hiyama, Sachin Gajghate, Irving  
38 M. Shapiro, and Makarand V. Risbud. PI3K/AKT Regulates Aggrecan Gene Expression  
39 by Modulating Sox9 Expression and Activity in Nucleus Pulposus Cells of the  
40 Intervertebral Disc. *J. Cell Physiol* (2009) 221; 668-676  
41  
42

43 [32] Schumacher BL, Su JL, Lindley KM, Kuettner KE, Cole AA. Horizontally oriented  
44 clusters of multiple chondrons in the superficial zone of ankle, but not knee articular  
45 cartilage. *Anat. Rec.* (2002). 266; 241-248  
46  
47

48 [33] Jadin KD, Wong BL, Bae WC, Li KW, Williamson AK, Schumacher BL, Price JH,  
49 Sah RL. Depth-varying density and organization of chondrocytes in immature and mature  
50 bovine articular cartilage assessed by 3d imaging and analysis. *J. Histochem. Cytochem.*  
51 (2005). 53; 1109-1119  
52  
53

54 [34] Clark JM, Rudd E. Cell patterns in the surface of rabbit articular cartilage revealed  
55 by the backscatter mode of scanning electron microscopy. *J. Orthop. Res.* (1991). 9; 275-  
56 283  
57  
58  
59  
60

1  
2  
3  
4  
5 [35] Rolauffs B, Williams JM, Grodinsky AJ, Kuettner KE, Cole AA. Distinct horizontal  
6 patterns in the spatial organization of superficial zone chondrocytes of human joints. *J.*  
7 *Struct. Biol.* (2008). 162; 335-344  
8

9 [36] Hakkinen L, Strassburger S, Kahari VM, Scott PG, Eichstetter I, Lozzo RV, Larjava  
10 H. A role for decorin in the structural organization of periodontal ligament. *Lab. Invest.*  
11 (2000) 80; 1869-1880  
12

13 [37] Matuszewski PE, Chen YL, Szczesny SE, Lake S, Elliot DM, Soslowsky LJ, Dodge  
14 GR. Regional variation in human supraspinatus tendon proteoglycans: decorin, biglycan,  
15 and aggrecan. *Connect. Tissue Res.* (2012). Jan 6 Epub ahead of print.  
16  
17

18 [38] Yang Qing-Hua, Song Yu-Peng, Jiang Haiyue, Zhuang Hong-Xing. The significance  
19 of the biomechanical properties of costal cartilage in the timing of ear reconstruction  
20 surgery. *J. of Plastic, Reconstructive and Aesthetic surgery* (2011). 64; 742-746  
21  
22

23 [39] Zhang G, Young BB, Ezura Y, Favata M, Soslowsky, Chakravarti S, Birk DE.  
24 Development of tendon structure and function: Regulation of collagen fibrillogenesis *J.*  
25 *Musculoskelet Neuronal Interact.* (2005) 5; 5-21  
26  
27

## TABLES

Table 1. A description of genes investigated in this study.

Gene	Name	Chromosome Location	Description
<i>ACTB</i>	$\beta$ -Actin	7p22	Housekeeping
<i>ACAN</i>	Aggrecan	15q26.1	Large aggregating proteoglycan
<i>BGN</i>	Biglycan	Xq28	Small proteoglycan (SLRP)
<i>CACNA1F</i>	Voltage-gated calcium channel- $\alpha$ 1F	Xp11.23	Voltage-sensitive calcium channel
<i>CAL1A1</i>	Collagen $\alpha$ -1 chain	17q21.33	Type I collagen fiber
<i>CAL2A1</i>	Collagen type II $\alpha$ -1	12q13.11	Type II collagen fiber
<i>DCN</i>	Decorin	12q21.33	Small proteoglycan (SLRP)
<i>FBN1</i>	Fibrillin 1	15q21.1	Large extracellular matrix glycoprotein
<i>NYX</i>	Nyctalopin	Xp11.4	Small proteoglycan (SLRP)
<i>SOX9</i>	SRY (Sex determining region Y)-box 9	17q24.3	Transcription regulator
<i>TGF<math>\beta</math>1</i>	Transforming Growth Factor- $\beta$ 1	19q13.2	Growth factor
<i>TIMP1</i>	Tissue inhibitor of metalloproteinase 1	Xp11.23	Inhibitor of matrix metalloproteinases

Table 2. Distribution of collagen fiber diameters in costal cartilage measured from SEM images.

<b>Fiber Dia.</b>	<b>0-0.09<math>\mu</math>m</b>	<b>0.1-0.99<math>\mu</math>m</b>	<b>1-9.9 <math>\mu</math>m</b>	<b>10-100 <math>\mu</math>m</b>
<b>% of total</b>	14.9	34	8.5	42.6
<b>Median</b>	0.08	0.426	1.036	21.5
<b>Range</b>	0.043-0.089	0.113-0.898	1.01-1.055	12.36-95.2

1  
2  
3  
4  
5  
6  
7  
8  
9  
10  
11  
12  
13  
14  
15  
16  
17  
18  
19  
20  
21  
22  
23  
24  
25  
26  
27  
28  
29  
30  
31  
32  
33  
34  
35  
36  
37  
38  
39  
40  
41  
42  
43  
44  
45  
46  
47  
48  
49

Table 3. Fold difference in gene expression (+/- SE) of four patients with pectus carinatum and an age-matched control compared to  $\beta$ -actin. Significant differences in expression between control and patients are marked with \*

	<b>Control</b>	<b>PC1</b>	<b>PC2</b>	<b>PC3</b>	<b>PC4</b>
<i>COL2A1</i>	134.0+/-7.06	134.31+/-49.33	*84.09+/-10.42	*46.96+/-12.22	118.79+/-10.24
<i>ACAN</i>	3.12+/-0.69	3.79+/-1.4	2.89+/-0.26	*1.30+/-0.15	*6.38+/-0.989
<i>DCN</i>	17.63+/-2.25	*4.47+/-0.51	*4.31+/-0.71	16.21+/-0.71	20.58+/-2.18
<i>TIMP1</i>	3.18+/-0.47	*0.67+/-0.07	*0.91+/-0.159	3.39+/-0.01	*5.53+/-0.46
<i>ACTB</i>	1	1	1	1	1
<i>BGN</i>	1.39+/-0.49	0.59+/-0.07	*0.33+/-0.09	0.84+/-0.01	*0.3+/-0.054
<i>COL1A1</i>	0.12+/-0.03	0.15+/-0.03	0.12+/-0.02	0.11+/-0.04	0.12+/-0.02
<i>FBN1</i>	0.46+/-0.08	NA	*0.18+/-0.01	0.49+/-0.05	0.30+/-0.15
<i>SOX9</i>	0.33+/-0.10	0.30+/-0.17	0.20+/-0.02	0.15+/-0.001	0.63+/-0.098
<i>TGF-<math>\beta</math>1</i>	0.18+/-0.09	0.15+/-0.021	0.13+/-0.041	0.09+/-0.016	0.04+/-0.005

Table 4. Gene expression ratios in costal cartilage from pectus carinatum and control. Published values are for cells of the lumbar nucleus pulposus (NP) and annulus fibrosus (AF) regions, and articular cartilage (AC), with references [ ].

	<i>COL2A1/ACAN</i>	<i>COL2A1/COL1A1</i>	<i>ACAN/COL1A1</i>	<i>DCN/BGN</i>
<b>PC1</b>	35.44	877.80	24.77	7.58
<b>PC2</b>	29.10	700.75	24.08	13.06
<b>PC3</b>	36.12	426.91	11.82	19.34
<b>PC4</b>	18.62	989.92	53.17	69.06
<b>Control</b>	42.95	1116.7	26	12.68
<b>Published</b>	23 NP [23] 370 AF [23] 1090 AC [23]	930 NP [23] 26 AF [23] 1790 AC [23]	4.6 <i>in vitro</i> [24] 78.4 sarcoma [24]	

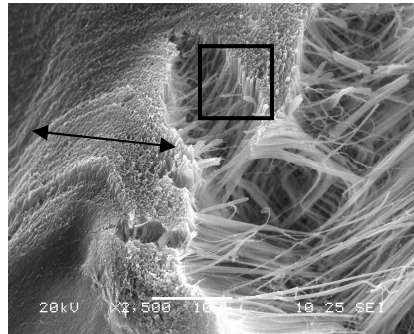


## Figure Legends

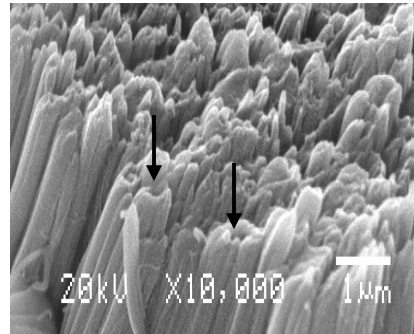
**Figure 1.** SEM and AFM images of normal costal cartilage. A. Transverse section (x2500) showing large numbers of dense fibrils running longitudinally (arrowed). B. Magnification (x10,000) of the boxed area in A and shows the presence of collagen nanostraws (arrowed). Each straw is approximately 650nm in diameter. C. Longitudinal section (x500) showing bundles of collagen fibers, formed from multiple collagen nanostraws, of approximately 20 $\mu$ m diameter (white arrow). D. Atomic force microscopy image of isolated collagen nanostraws of approximately 740nm maximal diameter (arrowed).

**Figure 2.** Localization of aggrecan by immunohistochemistry in transverse cross-sections of costal cartilage. A: Distribution of aggrecan in whole control section. B: Distribution of aggrecan in whole PC3 section. C-E: Distribution of aggrecan in control at 10x magnification from (C) periphery, (D) midzone, and (E) interior regions. Scale bars, 100  $\mu$ m. F-H: Distribution of aggrecan of aggrecan in control at 100x magnification from (F) periphery, (G) midzone, and (H) interior regions. Scale bars, 10  $\mu$ m. Notice the localization of aggrecan becomes more intense around each lacuna in the interior compared to the periphery.

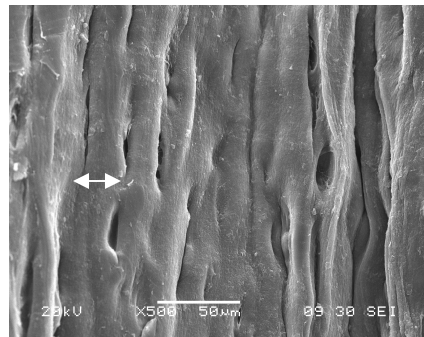
1a



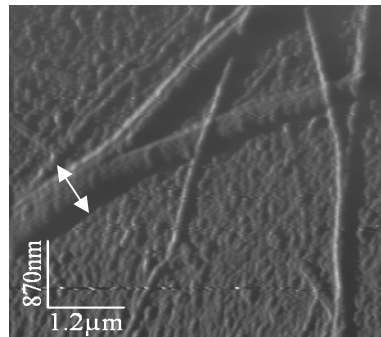
1b



1c



1d

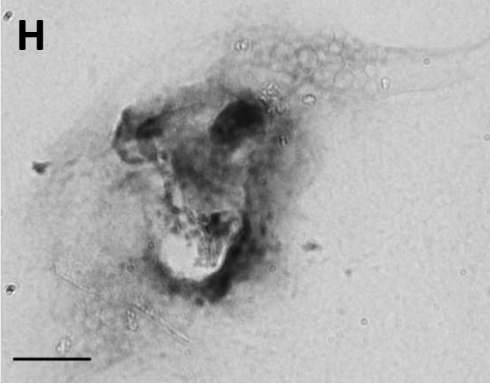
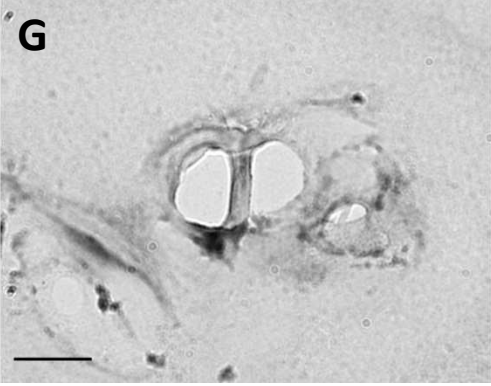
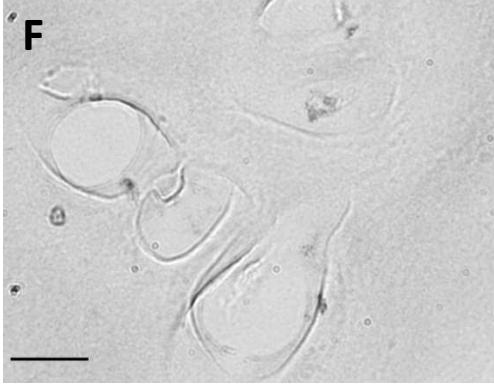
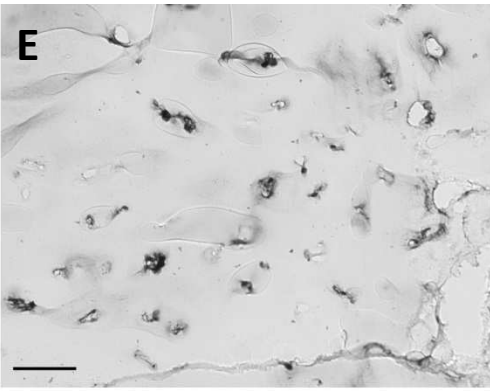
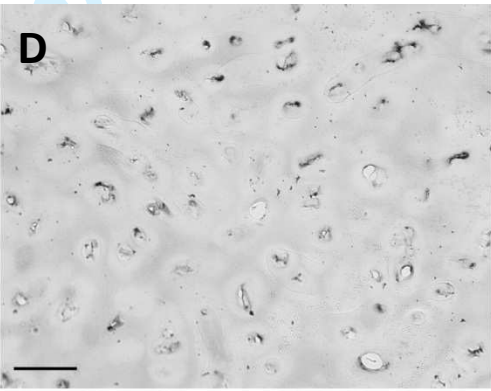
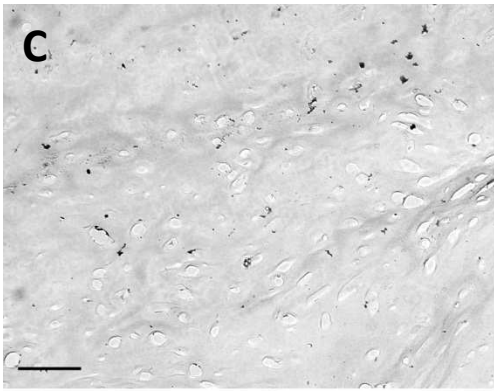
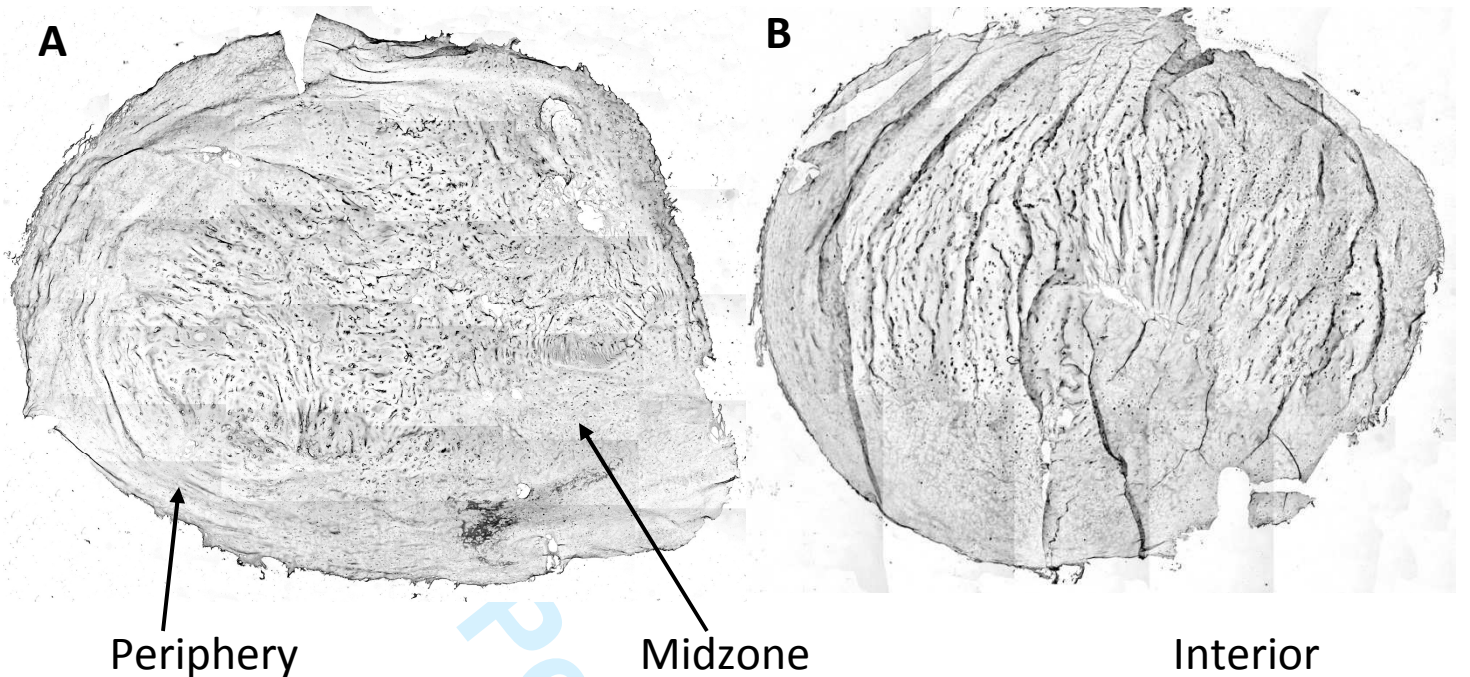


1  
2  
3  
4  
5  
6  
7  
8  
9  
10  
11  
12  
13  
14  
15  
16  
17  
18  
19  
20  
21  
22  
23  
24  
25  
26  
27  
28  
29  
30  
31  
32  
33  
34  
35  
36  
37  
38  
39  
40  
41  
42  
43  
44  
45  
46  
47  
48  
49

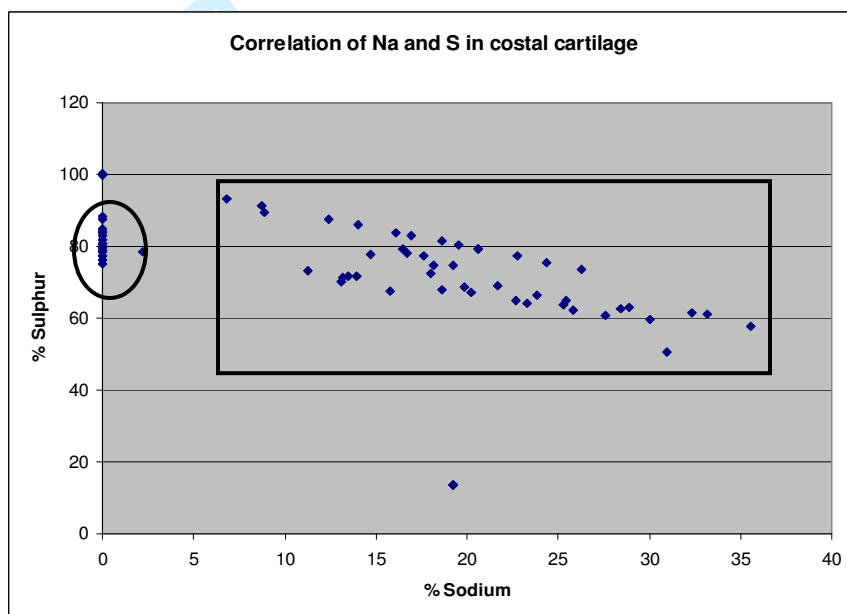
Control

PC3

1  
2  
3  
4  
5  
6  
7  
8  
9  
10  
11  
12  
13  
14  
15  
16  
17  
18  
19  
20  
21  
22  
23  
24  
25  
26  
27  
28  
29  
30  
31  
32  
33  
34  
35  
36  
37  
38  
39  
40  
41  
42  
43  
44  
45  
46  
47  
48  
49  
50  
51  
52  
53  
54  
55  
56  
57  
58  
59  
60



Supplemental Figure. Electron probe microanalysis of 100 equally spaced points over a transverse section of costal cartilage. Sodium is present only in the central 48 points (boxed), and not at the peripheral points, which contain Sulfur only (circled).



1  
2  
3  
4  
5  
6  
7  
8  
9  
10  
11  
12  
13  
14  
15  
16  
17  
18  
19  
20  
21  
22  
23  
24  
25  
26  
27  
28  
29  
30  
31  
32

**Decorin Expression, Straw-like Structure, and Differentiation of Human Costal Cartilage.**

Stacey MW<sup>1,2</sup>, Grubb J<sup>1</sup>, Asmar A<sup>1</sup>, Pryor J<sup>1</sup>, El-Sayed Ali<sup>3</sup> H, Cao W<sup>3</sup>, Beskok A<sup>4</sup>, Dutta D<sup>4</sup>, Darby DA<sup>5</sup>, Fecteau A<sup>6</sup>, Werner A<sup>7</sup>, Kelly RE Jr<sup>8</sup>.

<sup>1</sup>Frank Reidy Research Center for Bioelectronics, Old Dominion University, Norfolk, VA USA

<sup>2</sup>Department of Pediatrics, Eastern Virginia Medical School, Norfolk VA USA

<sup>3</sup> Applied Research Center, Electrical and Computer Engineering, Old Dominion University, Norfolk, VA

<sup>4</sup>Institute of Micro & Nanotechnology, Old Dominion University, Norfolk, VA

<sup>5</sup>Oceanography and Earth Sciences, Old Dominion University, Norfolk, VA

<sup>6</sup>Division of General Surgery, Hospital for Sick Children, Toronto, Canada.

<sup>7</sup>Dept of Pathology, Eastern Virginia Medical School and Med Director of Laboratories, Children's Hospital of The King's Daughters, Norfolk VA

<sup>8</sup> Department of Surgery, Eastern Virginia Medical School and Pediatric Surgery Division, Children's Hospital of the King's Daughters, Norfolk VA

33 Corresponding author:

34 Dr. Michael Stacey, Frank Reidy Research Center for Bioelectronics, 4211 Monarch Way,  
35 Suite 300, Norfolk, VA 23508 USA

36 Email: [mstacey@odu.edu](mailto:mstacey@odu.edu)

37 Telephone: 757 683 2245

38 Fax: 757 451 1010

39  
40  
41  
42  
43  
44  
45  
46  
47  
48  
49  
50  
51  
52  
53  
54  
55  
56  
57  
58  
59  
60

**Running head** Human costal cartilage

**Key Words** Pectus carinatum, chest wall deformities, connective tissue, SLRPs, AFM, gene ratio,

**ABSTRACT**

Costal cartilage is much understudied compared to the load bearing cartilages. Abnormally grown costal cartilages are associated with the inherited chest wall deformities pectus excavatum and pectus carinatum resulting in sunken or pigeon chest respectively. A lack of understanding of the ultrastructural and molecular biology of costal cartilage is a major confounder in predicting causes and outcomes of these disorders. The present study analyzed the structure of marginal human costal cartilage (ribs 6-10) through scanning electron and atomic force microscopy and identified the presence of straw-like structures running longitudinally. We also demonstrated that chondrocytes tend to occur singly or as doublets and that centrally located cells produce high levels of aggrecan compared to more peripherally located cells measured by immunohistochemistry. Gene expression from mRNA extracted from cartilage showed high levels of decorin expression, likely associated with the large, complex tubular structures running through this cartilage type. *COL2A1*, *ACAN* and *TIMP1* also showed higher levels of expression compared to *ACTB*. Analysis of gene expression ratios demonstrate that costal cartilage is under differentiated compared to published ratios for articular cartilage, likely due to the vastly different biomechanical environments of each cartilage type. Further studies need to establish whether findings described here from the costal margins are significantly different to cartilage of the 'true ribs' and how these values change with age.

## INTRODUCTION

Costal cartilage, a type of hyaline cartilage, connects each of ribs 1-5 to the sternum and ribs 6-10, which are fused, to the sternum as the costal margin. They remain cartilaginous throughout life and provide both strength and flexibility to the chest wall. Disorders of the chest wall can cause significant disfigurement with associated cardiac, pulmonary, and psychological manifestations and are classified as sunken chest (pectus excavatum, PE) or pigeon chest (pectus carinatum, PC) [1]. The costal cartilages of these patients are described as abnormally grown and weak. Disorders of costal cartilage are common, affecting approximately 1/400-1/1,000 individuals, show complex inheritance patterns in families, and affect primarily males (M4:F1) [2, 3, 4, 5]. Chest wall deformities are phenotypically variable and surgical repair outcomes can be unpredictable. The basic molecular characteristics that define a healthy human costal cartilage are largely unknown, and a lack of understanding of the ultrastructural and molecular biology of costal cartilage is a major confounder in predicting outcomes and causes chest wall deformities.

Recent work [6] described a decrease in the biomechanical stability of costal cartilage in pectus excavatum patients and suggested a disorderly arrangement and distribution of collagen fibers. Other authors have suggested that atypical collagen fibers may be implicated in chest wall deformities [7, 8]. The arrangement of collagen fibers in costal cartilage has not been described in detail; however, highly ordered fiber formation was described [9] in the surrounding perichondrium. Growth of human costal cartilage chondrocytes *in vitro* shows high levels of *COL2A1* and *ACAN* expression and low levels of *COL1A1* at low culture passage, typical of a differentiated cell [10]. Differences in the variable number of tandem repeat units of chondroitin sulphate attachment sites were observed in *ACAN* with significantly more repeats (27) being present in patients with chest wall deformities [11].

TGF $\beta$ 1 signaling plays a key role in cartilage growth and ECM turnover. Cells are extremely sensitive to levels of TGF $\beta$ 1 and, therefore, regulation of this growth factor is important in normal growth and development. Genes activated via TGF $\beta$  pathways include *SOX9*, a major transcription factor of chondrocyte differentiation and regulator of

**Deleted:** Cartilage tissue consists of chondrocytes and extracellular matrix (ECM) that primarily comprises collagens, small and large proteoglycans and water.

**Deleted:** an

**Deleted:** factor

**Deleted:** cartilage

1  
2  
3  
4  
5  
6  
7  
8  
9  
10  
11  
12  
13  
14  
15  
16  
17  
18  
19  
20  
21  
22  
23  
24  
25  
26  
27  
28  
29  
30  
31  
32  
33  
34  
35  
36  
37  
38  
39  
40  
41  
42  
43  
44  
45  
46  
47  
48  
49  
50  
51  
52  
53  
54  
55  
56  
57  
58  
59  
60

*ACAN* and *COL2A1* expression. In addition, *TIMP1*, a regulator of the matrix metalloproteinase's (MMP 8 and 13), is positively regulated by the TGFβ1 pathway [12].

Small leucine-rich proteoglycans (SLRPs) are small proteoglycans that are highly expressed in cartilage. Regulation of collagen fibrillogenesis is an important function shared by many SLRPs, and null mutations have been shown to lead to abnormal collagen architecture in mice [13]. Additionally, SLRPs mediate cell metabolism by binding to growth factors, including members of the superfamily TGFβ1 [14]. The causes of PE and PC are unknown; however, SLRPs can regulate ECM growth and fibrillogenesis by controlling TGFβ availability, suggesting a mechanistic role for SLRPs in these disorders. Biglycan deficiency has been shown to cause spontaneous aortic dissection and rupture in mice [15], and is also a characteristic of Marfan syndrome, a syndrome known to exhibit chest wall deformities. Decorin function is consistent with functions related to fibrillogenesis [16, 17]. A critical concept of SLRP function is compensation of one SLRP function over another. In the absence of biglycan, decorin is up-regulated and, therefore, differences in gene expression ratios may be apparent. Our central hypothesis is that abnormal expression of *BGN* and *DCN* will be observed in patients with chest wall deformities.

A thorough knowledge on the expression patterns of genes responsible for chondrogenesis in costal cartilage would provide insights into the role of these proteins in chest wall deformities and offer a biological rationale for the variability observed in outcome of surgery [18, 19, 20]. The objective of this study was to identify ultrastructural morphology and protein localization, investigate relative levels of expression of key genes required for chondrogenesis, and compare changes in normal costal cartilage and chest wall deformity.

## MATERIALS AND METHODS

### 2.1 Subjects

Human costal cartilage was obtained from 4 patients with pectus carinatum severe enough to warrant surgical repair. Informed consent was obtained following IRB approval of the protocol at Eastern Virginia Medical School. The IRB protocol currently prevents disclosure of many clinical features, and thus close correlation of clinical



1  
2  
3 phenotype with expression is not possible. Costal cartilage samples were collected from  
4 ribs 6-8 at surgery. Experiments were performed on the round, rod-like, mid-sections of  
5 cartilage. All patients were male, with an age range of early teen to early 20's.

**Deleted:** , cartilages that fuse and join ribs to the lower sternum as the costal margin

**Deleted:** described here

7 Apparently normal costal cartilage was obtained from an age-matched-control, a 15 year  
8 old male and processed within 24 hours. All samples were snap frozen in liquid nitrogen  
9 and stored at -80°C until use.

**Deleted:** from a recently deceased age-matched-control, a 15 year old male who died of unrelated causes

## 11 2.2 Ultrastructural analysis

13 Scanning electron microscopy (SEM) is a well-described technique employed for  
14 ultrastructural studies of cells and tissues. Cartilage samples were cut into small sections  
15 approximately 3mm thick, washed three times in Sorenson's buffer and digested at 37°C  
16 for 48 hours in trypsin (1mg/ml) and hyaluronidase (1mg/ml) in Sorenson's buffer [21].

**Deleted:** After surgical removal of costal c

17 Samples were washed thoroughly in PBS and fixed in 2.5% glutaraldehyde in phosphate  
18 buffered saline for 2.5 hours. Samples were rinsed in deionized water, dehydrated  
19 through an ethanol series, dried and mounted on carbon discs, gold sputtered, and  
20 examined using a JSM-6060LV SEM (JEOL, Tokyo, Japan) operating at 5 keV to  
21 minimize sample damage. Images were captured electronically and fiber measurements  
22 made using Image J software.

**Deleted:**

**Deleted:** to eliminate charge build-up during SEM analysis

**Deleted:** the low voltage of

**Deleted:** any

## 28 2.3 Atomic Force Microscopy (AFM)

29 Collagen straws were released from small pieces of tissue by brief homogenization and  
30 digestion with 0.1mg/ml hyaluronidase and 0.1mg/ml trypsin in Sorenson's buffer.  
31 Samples were fixed in ice cold acetone and fiber diameters measured using a Nanonics  
32 Multiview-4000 multi-probe AFM.

## 36 2.4 Immunohistochemistry

37 Confirmation of aggrecan gene expression and protein distribution were made by  
38 immunohistochemistry. Frozen cartilage samples were mounted in CRYO-OCT  
39 Compound (Tissue-Tek, CA USA) and sections (5µm) generated using a Microm  
40 HM525 cryostat. Sections were fixed in ice-cold acetone. Blocking, incubation with  
41 primary and secondary antibodies and washing were performed following manufacturer's  
42 guidelines for each antibody. Tissues were incubated with a mouse monoclonal antibody  
43 specific for aggrecan (sc-73693, Santa Cruz, Santa Cruz, CA). The antibody was raised  
44 against recombinant aggrecan from human origin. Negative controls were produced using

**Deleted:** Gene expression c

**Deleted:** confirmed for aggrecan

**Deleted:** (Santa Cruz Biotechnology, CA USA)

normal mouse IgG included in the ImmunoCruz mouse LSAB staining system (sc-2050, Santa Cruz). Electronic images were captured using a CCD camera through an Olympus BX51 with Metamorph and Image J software for semi and quantitative analysis of protein deposition.

**Deleted:** Detection was through horseradish peroxidase/DAB reaction using the ImmunoCruz staining system (Santa Cruz Biotechnology, CA USA).

## 2.5 Chondrocyte distribution

Cartilage consists mainly of proteoglycans and collagens, with chondrocytes sparsely distributed throughout the matrix. We catalogued the distribution pattern of 586 and 999 chondrocytes in transverse sections of costal cartilage from PC3 and Con3 respectively, through an Olympus BX51 microscope, as groups of 1-4+ cells per cluster located interiorly or peripherally. Interior cells were within the strongly expressing aggrecan region, and peripheral cells outside.

**Deleted:** 2

**Deleted:** of this

**Deleted:**

**Deleted:** and groups of 3 or more

**Formatted:** Superscript

## 2.6 Reverse Transcription and Real-Time PCR Analysis

Cartilage was removed from  $-80^{\circ}\text{C}$  and transverse sections cut at approximately 3-5mm on dry ice and placed into RNALater (Qiagen, CA USA). Samples were quickly weighed and approximately 100mg of costal cartilage was ground to a powder with a liquid nitrogen immersed pestle and mortar. RNA was isolated and genomic DNA eliminated by completing RNA extraction using a RNeasy Plus Mini Kit and RT-First Strand Kit (Qiagen, CA USA). All polymerase chain reactions (PCR) were performed on a BioRad CFX96 system in 25 $\mu\text{l}$  reactions using SYBR green detection (Qiagen, CA USA). Gene expression by PCR was performed on genes described in Table 1, all compared to the housekeeping gene *ACTB*. All primers were from Qiagen, CA USA. The reaction conditions were identical for all primers,  $95^{\circ}\text{C}$  for 10 minutes, then 40 rounds of  $95^{\circ}\text{C}$  for 15 seconds and  $60^{\circ}\text{C}$  for 60 seconds. Reaction specificities were assessed with a melt curve of  $65^{\circ}\text{C}$  to  $95^{\circ}\text{C}$  in  $0.2^{\circ}\text{C}$  increments. All experiments were in triplicate and performed with positive and negative controls. At least two independent extractions were included from samples stored at  $4^{\circ}\text{C}$  in RNALater. Data were standardized to housekeeping *ACTB* values for all samples using the delta Ct method.

**Deleted:** A

**Deleted:** Qiagen

**Comment [mws1]:** RNALater is a proprietary reagent stabilizes RNA and gave repeatable results within the time frame of our experiments. I can separate out the results, but I think this is more of a technical issue that may take away from the main thrust of the paper.

**Formatted:** Superscript

## 2.7 Statistical Analysis

Statistical analysis was performed using Student t-test to determine significance between sample and control means. For all tests,  $p < 0.05$  indicated the difference as significant.

## RESULTS

### 3.1. Electron Microscopy and AFM

Costal cartilage is a much understudied tissue type, both ultra structurally and genetically.

We provide a first description of these properties in samples of human costal cartilage.

Figures 1a and 1b are representative SEM images of a transverse cross-section of costal

cartilage taken from a mid-section. Figure 1a shows a fracture in the cartilage, estimated as the inner-middle zone, exposing collagen fibers of approximately 600nm diameter.

Fibers are assembled into extremely large complexes of many  $\mu\text{m}$  (arrowed) that run parallel to the length of the cartilage. Figure 1b is a higher magnification of the boxed

area and shows that each fiber forms a nanostraw of approximately 650nm external diameter and 250nm internal lumen diameter. Images of longitudinal sections show a well-defined organization of collagen fibers, approximately  $20\mu\text{m}$  diameter and cellular

lacunae (Figure 1c). We measured the diameters from 150 clearly defined fibers from SEM images (Table 2) and found that most were in the range from 0.1-100  $\mu\text{m}$ . The smallest ( $<0.1\mu\text{m}$ ) would most-likely represent the collagen fibrils, the midsize ( $\sim 1\mu\text{m}$ ) would represent the “microtubes” and the largest ( $\sim 100\mu\text{m}$ ) would be large fascicle-like structures. Cartilage homogenization and digestion released nanostraw fibers and allowed

further characterization by AFM. Figure 1d shows an AFM image of branching/splitting fibers with a maximum diameter of approximately 740nm. Clearly, costal cartilage has large fiber dimensions with complex structures formed through finely tuned fibrillogenesis.

### 3.2 Aggrecan immunohistochemistry

Aggrecan deposition from cells appeared to be a function of location. Figure 2 shows a representative cross-section of costal cartilage with cells located centrally exhibiting intense aggrecan staining (A) compared to the more peripherally located cells (B) and outer most cells (C). Interestingly, we were able to show increased levels of sodium ions in the same central region by electron probe microanalysis (EPMA, supplemental figure), showing that positively charged ions were drawn in to achieve electroneutrality.

### 3.3 Chondrocyte distribution

The organization of chondrocytes in cartilage is not considered to be random, and different cartilage types have different configurations of singles, pairs, clusters or strings

Deleted: t

Deleted: come

Deleted: together to form an

Deleted: with bundles

Deleted: of

Deleted: We measured diameters from 150 clearly defined fibers from SEM images and found measurements ranged from 43nm to 95.2 $\mu\text{m}$ . The distribution of diameter sizes is summarized in Table 1 and shows fibers are processed and packaged into thick fibrous structures.

Deleted: that are

of cells. The percentage number of cell clusters observed in the interior was 1 cell (68.5% and 60.2%), 2 cells (23% and 27.3%), 3 cells (4.3% and 10.1%) and 4+ cells (4.2% and 2.4%) respectively for PC3 and Control. For peripherally located cells, observed clusters were 1 cell (86.9% and 73.0%), 2 cells (12.6% and 19.7%), 3 cells (0.5% and 5.5%) and 4+ cells (0% and 1.8%) respectively for PC3 and Control. There is a trend towards higher cell clusters in the interior; however, there appears to be no differences in cell distribution between PC3 and age-matched control. No strings were observed.

**Deleted:** We did not find any apparent

**Deleted:** We observed over 90% of cells as singles or doublets in control (90.1%) and PC3 (95.4%) and only 1.04% and 1.08%, respectively, as clusters of 4 or more cells

### 3.4 Gene expression

Due to the unusual structure of costal cartilage we undertook analysis of gene expression to determine presence of the main constituents of cartilage; collagen type II, and the large aggregating proteoglycan, aggrecan. We also examined other genes that play a role in growth, structure and differentiation of cartilage. *BGN*, *NYX*, *CACNA1F* and *TIMP1* were of interest because these genes are located on the human X-chromosome, where affected individuals are predominantly male and possess only a single X-chromosome [2, 3].

**Deleted:** and may be significant in development of chest wall deformities

Costal cartilage from individuals with chest wall deformities is described as abnormally grown and weak. Typically, surgical repair takes place during teenage years to early 20's. Phenotypically, there is considerable variation of the clinical condition of PC, reflecting the complex nature and inheritance observed in these families. Variation in gene expression between samples is, therefore, expected; however, it is unknown whether the expression of matrix genes will be affected by surgical procedures. We compared gene expression of 4 patients with pectus carinatum to an age-matched-control. Table 3 shows *COL2A1*, *DCN*, *ACAN*, and *TIMP1* are all highly expressed compared to *ACTB*. Sample variation was noted, although, as expected, *COL2A1* was expressed to the highest level in all samples.

**Deleted:** expected

**Deleted:** Significant changes in gene expression are indicative of potential genetic influences on phenotype.

Compared to control, PC1 showed significant reduction in expression of *DCN* ( $p < 0.001$ ) and *TIMP1* ( $p < 0.001$ ). PC3 showed significantly lower expression of *COL2A1* ( $p < 0.001$ ) and like PC4, both showed decreased expression of *ACAN* ( $p < 0.03$  and  $p < 0.024$ , respectively). PC4 also showed significantly higher expression of *TIMP1* ( $p < 0.001$ ) and decreased expression of *BGN* ( $p < 0.04$ ). PC2 showed significant reduction in expression of *COL2A1* ( $p < 0.01$ ), *DCN* ( $p < 0.0002$ ), *TIMP1* ( $p < 0.001$ ), *BGN* ( $p < 0.03$ )

1  
2 and *FBNI* ( $p < 0.01$ ). This sample, like all PC samples, was immediately processed from  
3 the operating room, although results suggest possible degradation of this sample.

4  
5 Many patients with chest wall deformities are considered Marfanoid-like [22]  
6 without fulfilling all criteria for diagnosis of Marfan syndrome, including mutations of  
7 the fibrillin-1 gene. The expression of this gene was not significantly different between  
8 control and patients, with the exception of PC2 ( $p < 0.01$ ). Expression of the X-linked  
9 genes *NYX* and *CACNA1F* was not detected in any samples. Overall, deregulation of  
10 *TIMP1* expression was evident in 3/4 PC samples, and expression of *DCN* was  
11 significantly lower in 2/4, suggestive of roles for fibrillogenesis and matrix turnover. The  
12 differentiation status of cartilage can be equated to the ratio of *COL2A1*, present in  
13 differentiated cartilage, to *COL1A1*, present at higher levels in more undifferentiated  
14 cartilage. We compared ratios of gene expression to published data. Ratios of the  
15 differentiation markers *COL2A1:ACAN* and *COL2A1:COL1A1* are low in PC patients  
16 and control (Table 4) compared to rabbit articular cartilage (1090 and 1790, respectively)  
17 but both are highly comparable to the nucleus pulposus region of lumbar discs (23 and  
18 930 respectively), [23]. The ratios of *ACAN:COL1A1* fall between those reported for  
19 fully differentiated rat chondrosarcoma cells (78.4) and dedifferentiated chondrocytes  
20 cultured from costal cartilage (4.6) [24]. A high expression ratio of *COL2A1:COL1A1*  
21 (294.6) in human articular cartilage has been reported [25], but here results are referenced  
22 to *GAPDH* rather than *ACTB*. Overall, these results suggest costal cartilage is at an  
23 intermediate stage of differentiation and likely represents the different functional  
24 requirements of this tissue compared to articular cartilage. Small differences exist  
25 between patients and between patients and control (Table 4), suggesting that gene ratios  
26 measured here are not major contributors to chest wall abnormalities in these samples.  
27 Interestingly, *DCN* is expressed at high levels compared to *BGN*. As well as binding  
28 growth factors, both SLRPs have a role in fibrillogenesis and were hypothesized to play a  
29 role in the etiology of chest wall deformities. The high *DCN/BGN* ratio strongly suggests  
30 the importance of decorin expression in costal cartilage morphology. Decorin is present  
31 at high levels during tendon (fibro-cartilage) development and persists until thick fibers  
32 are formed [26], thus parallels with costal cartilage (hyaline cartilage) are apparent.  
33  
34  
35  
36  
37  
38  
39  
40  
41  
42  
43  
44  
45  
46  
47  
48  
49  
50  
51  
52  
53  
54  
55  
56  
57  
58  
59  
60

**Deleted:** To solidify this data, examination of further age-match controls and PC samples are required. ¶

## DISCUSSION

Costal cartilage is a much understudied cartilage where deformities have significant clinical consequences. A lack of understanding of molecular and ultrastructural properties hampers understanding events leading to these disorders. The present study compared relative gene expression of major genes of chondrogenesis from patients with pectus carinatum to an age-matched-control to answer questions relating to maintenance and differentiation. Perhaps the most important observations are 1) the longitudinal straw-like arrangement of collagen fibers, 2) the centrally located deposition of aggrecan, 3) the high level of decorin expression, and 4) gene ratios indicating under differentiation compared to articular cartilage.

The ultrastructural electron microscopy images show that human costal cartilage is unlike other cartilage types. Images appear to show that individual fibers are assembled to collectively form very thick, fascicle structures, appearing to consist of large numbers of collagen nanostraws that run parallel along the cartilage length. A similar observation of collagen tubules in juvenile rabbit tibia articular cartilage was reported [27], but this is the first report in human costal cartilage. The cartilage template of long bones is similar to costal cartilage in that they are both long, thick, rod-like structures and, therefore, although functionally different, ultrastructural similarities may be expected in response to cell maintenance and collagen fiber deposition under these conditions.

The morphological form of costal cartilage and how this relates to function is currently unknown. The presence of straw-like structures may provide strength and a means of gas and nutrient exchange to cells by fluid flow whose movement is dependent upon cartilage movement during breathing. Costal cartilage can be nearly 1cm diameter, outside of the range of diffusion to maintain centrally located cells [28]. Hypoxia or low pH has been shown to act as a trigger for aggrecan and collagen type II production through induction of hypoxia inducible factor 1- $\alpha$  and *SOX9*, as well as inhibit *COL1A1* expression [29, 30]. Similarities with inter vertebral discs are noteworthy. Cells embedded within the centrally located nucleus pulposus experience hypoxia and express aggrecan under the regulation of the hypoxia induced P13K/AKT signaling pathways via modulation of SOX9 [31]. It appears that as cells become centrally located

Deleted: come together

Deleted: . These structures

Deleted: a

Deleted: Interestingly, centrally located cells produce high levels of aggrecan.

Deleted: .

they experience hypoxia and lower pH. *ACAN* expression is induced with cationic uptake that we confirmed by Electron Probe Micro Analysis.

Deleted: in costal cartilage,

Deleted: and

Few studies have been undertaken on chondrocyte distribution within cartilage, yet cell density and arrangements are considered to be critical to function. Cellular clusters [32], pairs [33], and rows [34], have been reported. A more extensive study [35] in the superficial zone of articular cartilage identified complex patterns that appear to be location specific. A spatial relationship between collagen fiber alignment and cellular organization was suggested [34], with chondrocytes running parallel to adjacent fibers. Longitudinally, we also note the presence of lacunae between the large fibrous structures. The predominance of single and doublets in costal cartilage suggests cells undergo relatively few divisions. The absence of extensive strings and clusters is likely due to the different biomechanical forces experienced by costal cartilage compared to cartilage covering ball and socket joints.

Deleted: 1

Deleted: 2

Deleted: 3

Deleted: 4

Deleted: 3

SLRPs play an important role in fibrillogenesis and shape the architecture and mechanical properties of the collagen matrix. SLRP-deficient animals exhibit a wide array of diseases, mostly resulting from abnormal fibrillogenesis [13]. We examined the expression of three SLRPs; *DCN* and the X-linked genes *BGN* and *NYX*. *NYX* expression was not detected in any samples of costal cartilage and likely does not play a role in chondrogenesis. *DCN* has a role in modulating cartilage fibril growth, thickness, and orientation. Indeed, *DCN* deficiency introduces tissue-specific variations in range, mean, and distribution of collagen fibril diameters compared to wild-type. Interestingly, *DCN* deficiency also leads to random orientation of collagen fibrils in periodontal ligament instead of the usual parallel orientation [36]. Regional variation in localization of proteoglycans decorin, biglycan, and aggrecan has been reported in tendon, with decorin highest in regions of greatest tensile strength [37]. However, tensile strength of costal cartilage appears to reduce as it matures from childhood to teenage/early twenties years [38], suggesting rearrangement of collagen fibers with age that may be proteoglycan

Deleted: regulate the availability of growth factors and, taken together,

Deleted: 5

Deleted: 6

Deleted: 7

mediated. The highly aligned collagen fibers observed in costal cartilage show similarities to the aligned fibers of tendon. The hierarchical assembly of collagen fibers in tendon is a multistep process leading to the mature tissue [39]. Briefly, collagen fibril intermediates are assembled and undergo linear and lateral growth. Intercalation of fibrils

1  
2  
3  
4  
5  
6  
7  
8  
9  
10  
11  
12  
13  
14  
15  
16  
17  
18  
19  
20  
21  
22  
23  
24  
25  
26  
27  
28  
29  
30  
31  
32  
33  
34  
35  
36  
37  
38  
39  
40  
41  
42  
43  
44  
45  
46  
47  
48  
49  
50  
51  
52  
53  
54  
55  
56  
57  
58  
59  
60

is necessary for growth resulting in mature fibers and fibrils necessary for mechanical integrity. The interactions with fibril associated collagens and SLRPs have been implicated in the form and function of mature tendon. In costal cartilage an additional layer of complexity in the formation of tubules is intriguing, and, suggests, by the high level of *DCN* expression, that decorin is crucial in this morphology.

**Deleted:** The formation and orientation of straw-like structures observed in costal cartilage

**Deleted:** Alternatively, there is a possibility that *DCN* is being over expressed as a means of compensation for reduced expression of *BGN*.

**Deleted:** is

**Deleted:** are grown

**Deleted:** where *COL1A1* expression increases and *COL2A1* and *ACAN* expression decrease during dedifferentiation

The relative expression of genes expressed as a ratio has been used to determine differentiation status of cartilage where *COL2A1* and *ACAN* are highly expressed compared to *COL1A1*. This ratio decreases rapidly as chondrocytes dedifferentiate in vitro. Adaption of tissue to its mechanical constraints leads to different qualitative compositions. Costal cartilage exhibits a phenotype consistent with cartilage, with high *COL2A1/COL1A1*, *COL2A1/ACAN* and *ACAN/COL1A1* ratios, although *COL2A1/ACAN* and *COL2A1/COL1A1* ratios were considerably lower than rabbit articular cartilage also normalized to *ACTB* [24] suggesting *COL2A1* expression may be reduced. Expression levels in costal cartilage are closer to those reported in the nucleus pulposus of lumbar discs than to articular cartilage. Both nucleus pulposus and costal cartilage expression levels likely represent the functional requirements of their respective mechanical loads that are considerably different to that experienced in articular cartilage.

The present study has uncovered a new dimension of complexity that has not previously been reported. The study here describes findings that are generated from samples of costal cartilage that are generally removed at surgery, ribs 6-8. Although the current study has relatively few samples we feel that the overall results indicate that there are several important features unique to costal cartilage. Future work will examine variations along and between different ribs to more closely correlate variations of functions that may occur within the environment of the chest wall. Connective tissue gene arrays will allow analysis of many more genes simultaneously correlated to clinical picture. The etiology of chest wall deformity is complex. Changed growth characteristics of costal cartilage in patients may be a secondary characteristic due to external factors. Alternatively deformed cartilage may be intrinsic due to the inherited, albeit complex, nature of these disorders. Future work will aim to clarify these discrepancies.

## Acknowledgments



1  
2  
3  
4  
5  
6  
7  
8  
9  
10  
11  
12  
13  
14  
15  
16  
17  
18  
19  
20  
21  
22  
23  
24  
25  
26  
27  
28  
29  
30  
31  
32  
33  
34  
35  
36  
37  
38  
39  
40  
41  
42  
43  
44  
45  
46  
47  
48  
49  
50  
51  
52  
53  
54  
55  
56  
57  
58  
59  
60

We thank Dr M. Young, National Institute of Dental and Craniofacial Research, NIH and Dr C. Osgood, College of Sciences, Old Dominion University for critical review of this manuscript, and Old Dominion University Office of Research for seed funding grant.

**Declaration of interest:** The authors have declared no conflict of interest.

For Peer Review Only

**References**

- [1] Kelly RE, Shamberger RC, Mellins RB, Mitchell KK, Lawson ML, Oldham K, Azizkhan RG, Hebra AV, Nuss D, Goretsky MJ, Sharp RJ, Holcomb GW, Shim WKT, Megison SM, Moss RL, Fecteau AH, Colombani PM, Bagley TC and Moskowitz AB. Prospective Multicenter Study of Surgical Correction of Pectus Excavatum: Design, Perioperative Complications, Pain, and Baseline Pulmonary Function Facilitated by Internet-Based Data Collection. *J. Am. College of Surgeons.* (2007) 205: 205-216
- [2] Horth L, Stacey MW, Benjamin T, Segna K, Proud VK, Nuss D, Kelly RE. Genetic analysis of inheritance of *Pectus excavatum*. *J. Pediatric Genetics.* (2012) In press
- [3] Creswick H, Stacey M, Kelly R, Burke B, Gustin T, Mitchell K, Nuss D, Harvey H, Croitoru D, Goretsky M, Vasser E, Fox P, Goldblatt S, Tabangin M, Proud V. Family studies on the inheritance of pectus excavatum. *J. Pediatr. Surg.* (2006) 41:1699-1703
- [4] Leung AK, Hoo JJ. Familial congenital funnel chest. *Am. J. Med. Genet.* (1987). 26: 887-890
- [5] Sugiura, Y. A family with funnel chest in three generations. *Jpn. J. Hum. Genet.* (1977). 22: 287-289.
- [6] Feng J, Hu T, Liu W, Zhang S, Tang Y, Chen R, Jiang X, Wei F. The biomechanical, morphologic, and histochemical properties of the costal cartilages in children with pectus excavatum. *J. Pediatr. Surg.* (2001). 36: 1770-1776.
- [7] Rupprecht H, Hümmer, HP, Stöß, H, Waldherr T. Pathogenesis of the Chest Wall Deformities - Electron Microscope Studies and Analysis of Trace Elements in the Cartilage of the Ribs. *Eur J Pediatr Surg* (1987). 42(4): 228-229
- [8] Fokin AA, Nury M, Steuerwald M, Ahrens William A, Allen KE. Anatomical, Histologic, and Genetic Characteristics of Congenital Chest Wall Deformities. *Semin Thorac Cardiovasc Surg.* (2009). 21(1):44-57
- [9] Forman JL, del Pozo de Dios E, Dalmases CA, Kent RW. The contribution of the perichondrium to the structural mechanical behavior of the costal-cartilage. *J. Biomech. Eng.* (2010) 132; /094501 doi: 10.1115/1.4001976
- [10] Zhang Y, Chai G, Liu W, Cui L, Cao YL. Age-related changes in growth and metabolism function of human costal chondrocytes cultured in vitro. *Zhonghua Zheng Xing Wai Ke Zhi* (2004) 20; 372-376
- [11] Stacey M, Neumann S, Dooley A, Segna K, Kelly R, Nuss D, Kuhn A, Goretsky M, Fecteau A, Pastor A, Proud V. Variable Number of Tandem Repeat Polymorphisms (VNTRs) in the *ACAN* Gene Associated with Pectus Excavatum. *Clin. Genet.* (2010). 78;502-504

[12] El Mabrouk M, Qureshi HY, Li QW, Sylvester J, Zafarullah M. Interleukin-4 antagonizes oncostatin M and transforming growth factor beta-induced responses in articular cartilage. *J. Cell. Biochem.* (2008).103: 588-597.

[13] Ameye L, Young MF. Mice deficient in small leucine-rich proteoglycans: novel in vivo models for osteoporosis, osteoarthritis, Ehlers-Danlos syndrome, muscular dystrophy, and corneal diseases. *Glycobiology* (2002).12: 107R-116R.

[14] Hildebrand A, Romaris M, Ramussen LM, Heingard D, Twardzik DR, Border WA, Ruoslahti E Interaction of the small interstitial proteoglycans biglycan, decorin and fibromodulin with transforming growth factor  $\beta$ . *Biochem. J.* (1994). 302: 527-534

[15] Heegaard AM, Corsi A, Danielsen CC, Nielsen KL, Jorgensen HL, Riminucci M, Young MF, Bianco P. Biglycan Deficiency Causes Spontaneous Aortic Dissection and Rupture in Mice. *Circulation.* (2007);115:2731-2738.

[16] Bianco P, Fisher LW, Young MF, Termine JD, Robey PG. Expression and localization of the two small proteoglycans biglycan and decorin in developing human skeletal and non-skeletal tissues. *J. Histochem. Cytochem.* (1990). 38: 1549-1563

[17] Kalamajski S, Oldberg A. The role of small leucine-rich proteoglycans in collagen fibrillogenesis. *Matrix Biol.* (2010) 29; 248-253

[18] Antonoff MB, Saltzman DA, Hess DJ, Acton RD. Retrospective review of reoperative pectus excavatum repairs. *J. Pediatr Surg.* (2010). 45(1):200-5.

[19] Bouchard S, Hong AR, Gilchrist BF, Kuenzler KA. Catastrophic cardiac injuries encountered during the minimally invasive repair of pectus excavatum. *Semin. Pediatr. Surg.* (2009) 18(2):66-72.

[20] Swanson JW, Colombani PM. Reactive pectus carinatum in patients treated for pectus excavatum. *J. Pediatr. Surg.* (2008). 43(8):1468-73.

[21] [Stolz M, Gottardi R, Raiteri R, Miot S, Martin I, Imer R, Stauffer U, Raducanu A, Düggelein M, Baschong W, Daniels AU, Friederich NF, Aszodi A & Aebi U. Early detection of aging cartilage and osteoarthritis in mice and patient samples using atomic force microscopy. \*Nature Nanotechnology\* \(2009\) 4; 186-192](#)

Deleted: ¶

Formatted: Space Before: 0 pt, After: 0 pt, Line spacing: single

[22] [Redlinger RE Jr., Rushing GD, Moskowitz AD, Kelly RE, Jr., Nuss D, Kuhn A, Obermeyer RJ, Goretsky MJ. Minimally invasive repair of pectus excavatum in patients with Marfan Syndrome and Marfanoid features. \*J. Pediatr. Surg.\* \(2010\). 45\(1\): 193-199](#)

Deleted: Goldring MB, Goldring SR. Osteoarthritis. *J. Cell. Physiol.* (2007). 213; 626-634¶

[23] Clouet J, Grimandi G, Pot-Vaucel M, Masson M, Fellah HB, Guigand L, Chérel Y, Bord E, Rannou F, Weiss P, Guicheux J and Vinatier C. (2009). Identification of phenotypic discriminating markers for intervertebral disc cells and articular chondrocytes. *Rheumatology* (2009) 48 (11): 1447-1450.

[24] McAlinden A, Havlioglu N, Liang L, Davies SR, Sandell LJ. Alternative Splicing of Type II Procollagen Exon 2 Is Regulated by the Combination of a Weak 5' Splice Site and an Adjacent Intronic Stem-loop Cis Element. *J. Biol. Chem.* (2005). 280; 32700-32711

[25] Martin I, Jakob M, Schafer D, Dick W, Spagnoli G, Heberer M. Quantitative analysis of gene expression in human articular cartilage from normal and osteoarthritic joints. *Osteoarthr. Cartilage* (2001) 9; 112-118

[26] Kalamajski S, Oldberg A. The role of small leucine-rich proteoglycans in collagen fibrillogenesis. *Matrix Biology* (2010) 29; 248-253

[27] Gwynn AP, Wade S, Kääh MJ, Owen GR, Richards RG. Freeze-substitution of rabbit tibial articular cartilage reveals that radial zone collagen fibers are tubules. *J. Microsc.* (2000) 197; 159-172

[28] Gibson JS, Milner PI, White R, Fairfax TP, Wilkins RJ. Oxygen and reactive oxygen species in articular cartilage: modulators of ionic homeostasis. *Pflugers Arch.* (2008) 455; 563-573

[29] Duval E, Leclercq S, Elissalde JM, Demoor M, Galera P, Boumediene K. Hypoxia-inducible factor 1 $\alpha$  inhibits the fibroblast-like markers type I and type III collagen during hypoxia-induced chondrocyte redifferentiation. *Arthritis Rheum.* (2009) 60; 3038-3048

[30] Das RHJ, van Osch GJVM, Kreukniet M, Oostra J, Weinans H, Jahr H Effects of individual control of pH and hypoxia in chondrocyte culture. *J. Orthop. Res.* (2010). 28; 537-545

[31] [Chin-Chang Cheng, Yoshiyasu Uchiyama, Akihiko Hiyama, Sachin Gajghate, Irving M. Shapiro, and Makarand V. Risbud. PI3K/AKT Regulates Aggrecan Gene Expression by Modulating Sox9 Expression and Activity in Nucleus Pulposus Cells of the Intervertebral Disc. \*J. Cell Physiol\* \(2009\) 221; 668-676](#)

[32] Schumacher BL, Su JL, Lindley KM, Kuettner KE, Cole AA. Horizontally oriented clusters of multiple chondrons in the superficial zone of ankle, but not knee articular cartilage. *Anat. Rec.* (2002). 266; 241-248

[33] Jadin KD, Wong BL, Bae WC, Li KW, Williamson AK, Schumacher BL, Price JH, Sah RL. Depth-varying density and organization of chondrocytes in immature and mature bovine articular cartilage assessed by 3d imaging and analysis. *J. Histochem. Cytochem.* (2005). 53; 1109-1119

[34] Clark JM, Rudd E. Cell patterns in the surface of rabbit articular cartilage revealed by the backscatter mode of scanning electron microscopy. *J. Orthop. Res.* (1991). 9; 275-283

Formatted: Normal

Formatted: Line spacing: single

Formatted: Normal

Deleted: ¶

Deleted: 1

Deleted: 2

Deleted: 3

[35] Rolauffs B, Williams JM, Grodinsky AJ, Kuettner KE, Cole AA. Distinct horizontal patterns in the spatial organization of superficial zone chondrocytes of human joints. *J. Struct. Biol.* (2008). 162; 335-344

Deleted: 4

[36] Hakkinen L, Strassburger S, Kahari VM, Scott PG, Eichstetter I, Lozzo RV, Larjava H. A role for decorin in the structural organization of periodontal ligament. *Lab. Invest.* (2000) 80; 1869-1880

Deleted: 5

[37] Matuszewski PE, Chen YL, Szczesny SE, Lake S, Elliot DM, Soslowsky LJ, Dodge GR. Regional variation in human supraspinatus tendon proteoglycans: decorin, biglycan, and aggrecan. *Connect. Tissue Res.* (2012). Jan 6 Epub ahead of print.

Deleted: 6

[38] Yang Qing-Hua, Song Yu-Peng, Jiang Haiyue, Zhuang Hong-Xing. The significance of the biomechanical properties of costal cartilage in the timing of ear reconstruction surgery. *J. of Plastic, Reconstructive and Aesthetic surgery* (2011). 64; 742-746

Deleted: 7

[39] Zhang G, Young BB, Ezura Y, Favata M, Soslowsky, Chakravarti S, Birk DE. Development of tendon structure and function: Regulation of collagen fibrillogenesis *J. Musculoskelet Neuronal Interact.* (2005) 5; 5-21

Deleted: ¶  
¶

Formatted: Line spacing: single

Deleted: Chin-Chang Cheng, Yoshiyasu Uchiyama, Akihiko Hiyama, Sachin Gajghate, Irving M. Shapiro, and Makarand V. Risbud. PI3K/AKT Regulates Aggrecan Gene Expression by Modulating Sox9 Expression and Activity in Nucleus Pulposus Cells of the Intervertebral Disc. *J. Cell Physiol* (2009) 221; 668-676¶  
Stolz M, Gottardi R, Raiteri R, Miot S, Martin I, Imer R, Stauffer U, Raducanu A, Duggelin M, Baschong W, Daniels AU, Friederich NF, Aszodi A & Aebi U. Early detection of aging cartilage and osteoarthritis in mice and patient samples using atomic force microscopy. *Nature Nanotechnology* (2009) 4; 186-192¶